Atomistic Simulation of Creep in a Nanocrystal

Timothy T. Lau,[1] Akihiro Kushima,[2] and Sidney Yip[1,2,*]

[1]Department of Materials Science and Engineering, Massachusetts Institute of Technology, Cambridge, Massachusetts 02139 USA
[2]Department of Nuclear Science and Engineering, Massachusetts Institute of Technology, Cambridge, Massachusetts 02139 USA

(Received 24 June 2009; revised manuscript received 29 March 2010; published 27 April 2010)

We describe a method to simulate on macroscopic time scales the stress relaxation in an atomistic nanocrystal model under an imposed strain. Using a metadynamics algorithm for transition state pathway sampling we follow the full evolution of a classical anelastic relaxation event, with relaxation times governed by the nanoscale microstructure imperfections in the solid. We show that probing this sensitive variation leads to mechanistic insights that reveal a direct correlation between system-level relaxation behavior and localized atomic displacements in the vicinity of the nanostructured defects, in turn implying a unit mechanism for self-organized plastic response. This suggests a new class of measurements in which the microstructure imperfections are characterized and matched to predictive simulations enabled by the present method.

DOI: 10.1103/PhysRevLett.104.175501 PACS numbers: 62.20.Hg, 68.35.bd, 83.85.St

It is well known that molecular dynamics (MD) and related atomistic methods for probing dynamical processes are restricted to microscopic time scales [1]. While MD studies of creep deformation have resorted to high temperature [2], high stress [3], and high applied strain [4], the strain rates are nevertheless of the order 10^7 s^{-1}, and the challenge of dealing with microstructural evolution in the time range from seconds to years remains. Here we propose an approach based on activated-state kinetics and demonstrate its potential in mediating the strain-rate bottleneck in atomistic simulations.

Our work is motivated by a recent atomistic study of supercooled liquids where the shear viscosity was computed over 18 orders of magnitude [5]. This calculation was enabled by an algorithm, to be called autonomous basin climbing (ABC), that drives a bulk system of interacting particles to climb out of any local potential energy minimum by a series of activation-relaxation steps. ABC is an adaptation of the metadynamics approach to energy landscape sampling [6,7]; it is equally applicable to probe structural relaxation in systems under an applied strain. We demonstrate this in a nanocrystal model of spherical grains. We used transition state theory to translate each activation energy in the transition state pathway trajectory sampled by ABC into an elapsed time for the associated structural evolution event, thus generating the time response of the stress relaxation in the spirit of the theory of anelastic solids [8]. For the atomistic simulation to make contact with mechanical spectroscopy experiments [9], two effects are found to be important, variation with applied strain and microstructure imperfections of the sample. While the former can be reasonably treated by direct scaling, the latter is an issue that has not been addressed in previous simulation studies. We find the characteristic anelastic relaxation time to be highly sensitive to the atomic-level ''defect structures'' such as a nm-sized void or a distribution of monovacancies, to the extent that comparison between simulation and experiment depends critically on controlling these defects in the experimental specimens. We believe this to be the first atomistic simulation of deformation on macroscopic time scales that reveals the underlying atomic-level unit process for plastic deformation in small volumes.

Our model system is a 3D construction of spherical grains arranged in a periodic bcc array. A slow cool was conducted with MD on a melt embedded with two small seeds of bcc Fe atoms, producing a nanocrystal of two approximately spherical grains, each 29.8 Å in diameter, containing in total $N = 3456$ atoms [Fig. 1(a)]. Figure 1(b) shows the intergranular versus intragranular portions of the cell, the atom number ratio being 60%. A prescribed tensile strain in the z direction is imposed on the initially relaxed system after which energy minimization is performed on all the atomic coordinates and the x and y cell dimensions.

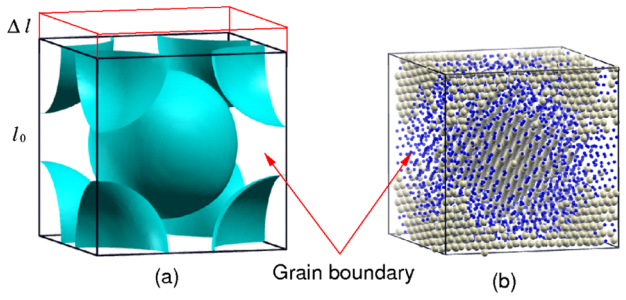

FIG. 1 (color online). The periodic simulation cell in two renderings. (a) Only the two spherical grains are shown while all the atoms occupying the grain boundary space are suppressed. (b) All atoms are shown, larger size (pale [light gray]) form the grain interior, while smaller size (blue [dark gray]) delineate the grain-boundary region according to a central-symmetry criterion. Imposed strain ε is defined by the ratio Δl to l_0.

Transition state pathway sampling runs are then conducted with the new cell dimensions held constant.

The ABC algorithm begins with an activation step in which a $3N$-dimensional Gaussian penalty function is added to the existing potential energy surface. We employ a Finnis-Sinclair empirical potential for the interatomic interactions [10]. The penalty has the effect that, upon minimization of the combined energy, penalty plus the original potential, the system is pushed away from its initial configuration into a higher energy state. The cycle is repeated by adding a new penalty. After a series of activation and relaxation steps, the system crosses an energy saddle point during a relaxation step and settles into an adjacent well. Since the imposed penalty functions are not removed, the system is discouraged from returning to any of the previously visited potential minima.

The output of our simulation is a set of transition state pathway trajectories, each being an ordered sequence of energy minima and saddle points [5]. We estimate the elapsed time Δt of each activation-relaxation event, with its corresponding structural deformation, using transition state theory [11]

$$\Delta t = \left[\nu_0 \exp\left(-\frac{\Delta U}{k_B T}\right)\right]^{-1} \tag{1}$$

where ΔU is the saddle point energy relative to the previous local minimum, ν_0 is a characteristic frequency factor (taken to be 10 THz), and T is the temperature. This relation allows us to correlate the stress at any point on the trajectory with a total elapsed time, the sum of the individual elapsed times for each preceding activation-relaxation event along the trajectory, thus yielding a time-dependent stress relaxation curve. Implicit in this mapping procedure is the assumption that the individual events are not correlated, a fundamental hypothesis in the theory of anelastic deformation [8].

The stress relaxation results are displayed in a log-linear plot, Fig. 2. The simulation data, shown as symbols, are fitted to a traditional empirical anelastic relaxation expression [8,12],

$$\frac{\sigma(t)}{\varepsilon_0} = M_R + (M_U - M_R)\exp\left(-\frac{t}{\tau}\right) \tag{2}$$

where ε_0 is the constant applied strain, M_R and M_U are the relaxed and unrelaxed stresses, respectively. Within the fluctuations of the simulation data, one sees that the full evolution of an anelastic relaxation process is captured, from a significant incubation period for structural rearrangements before the manifestation of stress relaxation to a final value. In the range of strain studied the relaxations occur over time periods from 10^7 to 10^{11} s, a range well beyond the reach of molecular dynamics simulation. The effective relaxation times τ obtained from the fitting are found to vary with the imposed strain in an essentially exponential manner, $\log(\frac{\tau}{s}) = 185.07\varepsilon_0 + 7.0131$. That relaxation occurs at later times for larger initial strains may appear counterintuitive; it can be explained by noting a greater driving force gives rise to larger activation volume (see below) which requires longer time for self-organization to dissipate the built-up stress. The relaxation times obtained in Fig. 2 are considerably longer than what has been observed experimentally, $\tau \sim 10^3$ s. One should not be surprised by this difference in view of the pristine nature of the nanocrystyal model used in the simulation. It is to be expected that the actual experimental specimens used have a higher content of microstructure imperfections than the structure seen in Fig. 1. To probe the sensitivity of the relaxation to these nanoscale imperfections we have performed additional simulations where two types of defects were introduced into the grain-boundary region delineated in Fig. 1. One was a single void of 0.3 nm and the other was a distribution of vacancies (removing one atom out of every ten). Simulations were run at an imposed strain of $\varepsilon = 0.02$ and 400 K. The resulting stress relaxation profiles were very different from those shown in Fig. 2. In the case of void insertion, stress relaxation occurred very quickly, with τ reduced to 10^{-8} s. In the case of the vacancy insertion, σ/ε_0 was reduced by a factor of 3 and τ reduced to 10^4 s. We can attribute the τ reduction by 16 orders of magnitude to the free volume of the void which allows atoms to move ballistically and thus relax the stress. The reduction of τ in the case of vacancy distribution is an interesting finding in that the relaxation time is now in the

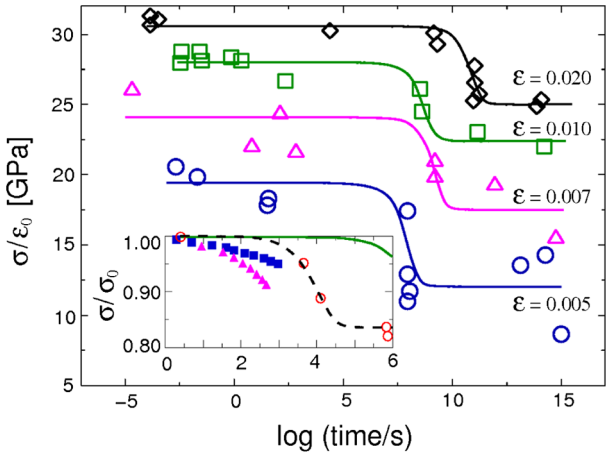

FIG. 2 (color online). Temporal evolution of von Mises stresses at 400 K and various applied strains, with the stress at zero applied strain subtracted and normalized by the applied strain. Each data point represents a weighted average of the calculated stress within a 0.01 interval of log (time/s). Simulation data are shown as circles ($\varepsilon = 0.005$), triangles ($\varepsilon = 0.007$), squares ($\varepsilon = 0.010$), diamonds ($\varepsilon = 0.020$). Solid lines are results of fitting to Eq. (2). Inset shows comparison of experimental data at strain of 0.0002 for "as-prepared" (triangles) and "annealed" (squares) samples at 313 K and 408 K respectively [9], with scaled simulation results of the pristine nanocrystal (solid line) and the distributed-vacancy (dashed line) models at 400 K.

range of experiments [9], implying that effectively this level of microstructure imperfections in the simulation is a reasonable match with the nanoscale defects in the physical specimens. In the Fig. 2 inset we show a comparison with experiments using two specimens, as prepared and annealed [9], of the simulation results for the vacancy distribution case, extrapolated to the same strain level of $\varepsilon = 0.002$. Judging from the effects of the different specimens, one could see experiments approaching simulation if specimens that are more pristine than those used were available. For quantitative comparison between simulation and experiment, both must probe the same range of stress relaxation times. To our knowledge this is the first deformation simulation with full atomistic configuration details to reach the time scale of creep experiments.

Since each relaxation curve in Fig. 2 is obtained from a corresponding transition state pathway trajectory, detailed inspection of the trajectories offer insights into the underlying atomic-level mechanisms. As shown in Fig. 3(a), two features appear in each trajectory, a continuous background of small-energy oscillations (not readily visible at the scale displayed), and an intermittent relatively large-energy relaxation (indicated by arrows). We will refer to these features as "serrated" and "drop" modes of response, respectively. The atomic configurations immediately after two drop events [arrows in Fig. 3(a)], are shown in Figs. 3(b) and 3(c) for the two applied strains. One sees the system response is essentially due to atomic mobility confined to the grain-boundary region. Moreover, imposing a larger strain leads to a broader distribution of activated sites, or effectively a larger activation volume. Thus we can interpret the longer effective relaxation time seen in Fig. 2 to signify longer time for the plastic deformation to be organized and manifest. Combining Figs. 2 and 3 we find the underlying mechanism responsible for the system-level stress relaxation on macroscopic time scales to involve both serrated and drop modes, the former being distributed and continuous while the latter are localized and intermittent. It is the series of discrete "unit processes" that enable the system to self-organize and undergo significant plastic deformation. Additionally it should be mentioned that discrete energy or stress drops have been reported and analyzed in previous atomistic simulations of structural deformation, for example, in the load-displacement curve in nanoindentation of a metal thin film [13], also seen experimentally, in the stress-strain curve of an analog of metallic glasses [14], and in the shear deformation of a molecular model of cement [15]. They appear to be universal behavior characteristic of deformation in small volumes, independent of structural order (crystal versus amorphous) or method of simulation (metadynamics versus molecular dynamics).

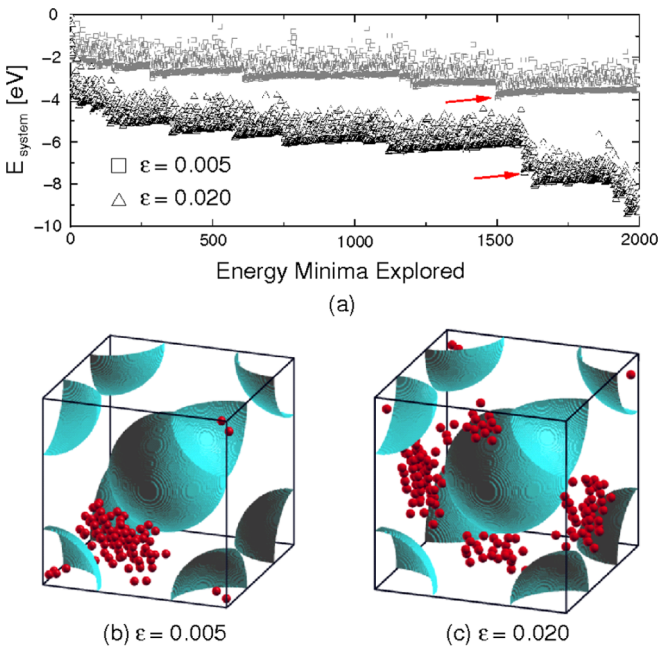

FIG. 3 (color online). (a) Variation of potential energy of the simulation cell as the system undergoes stress relaxation at constant strain of 0.005 and 0.020 as sampled by the algorithm ABC. (b) Cluster of active atoms associated with the energy drop event indicated by the arrow at 0.005 strain in (a); these atoms have undergone displacement greater than 0.1 Å when comparing atomic configurations just before and after the energy drop event. (c) same as (b) except for strain 0.020. Figures generated with XCrySDen [25].

Using a novel method of sampling potential energy surfaces to study stress relaxation in a model nanocrystal, we demonstrate an ability of atomistic simulations to probe macroscopic time scales, while providing access to atomic configuration details. We show the underlying mechanism involves the discrete, localized irreversible atomic displacements analogous to those observed in molecular dynamics simulations at strain rates many orders of magnitude higher. Given our findings on the dominant role of microstructure imperfections at the nanoscale, one can conclude that experimental test of our method of simulating creep deformation will require the availability of specimens with defect structures effectively matching those of the simulation. This may be feasible with recent advances in experimental techniques, such as field ion beam fabrication of nanopillars and nanoindentation measurement of small-scale yielding [16–18]. A new class of experiments could emerge where nanoscale plastic deformation measurements are coupled to predictive atomistic simulations [19,20] extended to include the present method. The ability to correlate atomistic details of microstructural evolution with system-level relaxation at long times should broaden the range of physical phenomena that can be usefully explored by atomistic simulations. It could lead to new perspectives on MD-based studies such as cooperative atomic rearrangements in supercooled liquids under shear [21], distribution of plastic strains in metallic glass [22], surface dislocation nucleation on a nanowire

[23], and extrusion of single nanocrystals from graphitic capsulus [24].

We gratefully acknowledge support from the U.S. National Defense Science and Engineering program (T. T. L.), SKF Global, Inc., Corning Incorporated, and HondaR&D, Inc., and discussions with A. S. Argon, Wei Cai, J. R. Greer, and M. Kassner.

*Corresponding author. syip@mit.edu

[1] A. F. Voter, F. Montalenti, and T. C. Germann, Annu. Rev. Mater. Res. **32**, 321 (2002).
[2] V. Yamakov, D. Wolf, S. R. Phillpot, and H. Gleiter, Acta Mater. **50**, 61 (2002).
[3] H. Van Swygenhoven, M. Spaczer, A. Caro, and D. Farkas, Phys. Rev. B **60**, 22 (1999).
[4] J. Schiøtz, T. Vegge, F. D. Di Tolla, and K. W. Jacobsen, Phys. Rev. B **60**, 11971 (1999).
[5] A. Kushima, X. Lin, J. Li, X. Qian, J. Eapen, J. C. Mauro, P. Diep, and S. Yip, J. Chem. Phys. **130**, 224504 (2009).
[6] A. Laio and M. Parrinello, Proc. Natl. Acad. Sci. U.S.A. **99**, 12 562 (2002).
[7] A. Laio and F. L. Gervasio, Rep. Prog. Phys. **71**, 126601 (2008).
[8] A. S. Nowick and B. S. Berry, *Anelastic Relaxation in Crystalline Solids* (Academic Press, Inc., New York, 1972).
[9] E. Bonetti, E. G. Campari, L. Del Bianco, L. Pasquini, and E. Sampaolesi, Nanostruct. Mater. **11**, 709 (1999).
[10] T. T. Lau, C. J. Först, X. Lin, J. D. Gale, S. Yip, and K. J. Van Vliet, Phys. Rev. Lett. **98**, 215501 (2007).
[11] G. H. Vineyard, J. Phys. Chem. Solids **3**, 121 (1957).
[12] M. E. Kassner, *Fundamentals of Creep in Metals and Alloys* (Elsevier, Amsterdam, 2009), 2nd ed..
[13] J. Li, K. J. V. Vliet, T. Zhu, S. Suresh, and S. Yip, Nature (London) **418**, 307 (2002).
[14] A. S. Argon and M. J. Demkowicz, Metall. Mater. Trans. A **39**, 1762 (2008).
[15] R. J. M. Pellenq, A. Kushima, R. Shahsavari, K. J. V. Vliet, M. Buehler, S. Yip, and F. Ulm, Proc. Natl. Acad. Sci. U.S.A. **106**, 16 102 (2009).
[16] M. D. Uchic, D. M. Dimiduk, J. N. Florando, and W. D. Nix, Science **305**, 986 (2004).
[17] J. R. Greeer, W. C. Oliver, and W. D. Nix, Acta Mater. **53**, 1821 (2005).
[18] D. M. Dimiduk, M. D. Uchic, and T. A. Parthasarathy, Acta Mater. **53**, 4065 (2005).
[19] C. R. Weinberger and W. Cai, Proc. Natl. Acad. Sci. U.S.A. **105**, 14 304 (2008).
[20] C. R. Weinberger and W. Cai, Nano Lett. **10**, 139 (2010).
[21] A. Furukawa, K. Kim, S. Saito, and H. Tanaka, Phys. Rev. Lett. **102**, 016001 (2009).
[22] D. Rodney and C. Schuh, Phys. Rev. Lett. **102**, 235503 (2009).
[23] T. Zhu, J. Li, A. Samanta, A. Leach, and K. Gall, Phys. Rev. Lett. **100**, 025502 (2008).
[24] S. Suresh and J. Li, Nature (London) **456**, 716 (2008).
[25] A. Kokalj, Comput. Mater. Sci. **28**, 155 (2003).